Microb Ecol (2011) 62:518–527
DOI 10.1007/s00248-011-9852-5

ENVIRONMENTAL MICROBIOLOGY

Isolation and Characterization of Exopolysaccharide Secreted by a Toxic Dinoflagellate, *Amphidinium carterae* Hulburt 1957 and Its Probable Role in Harmful Algal Blooms (HABs)

Subir Kumar Mandal · Ravindra Pal Singh · Vipul Patel

Received: 31 December 2010 / Accepted: 21 March 2011 / Published online: 19 April 2011

Abstract Extracellular polymeric substances (EPS) produced by a toxic dinoflagellate *Amphidinium carterae* Hulburt 1957 was isolated and characterized. Molecular masses of the EPS were about 233 and 1,354 kDa. Spectral analyses by ^{1}H nuclear magnetic resonance and Fourier Transformed–Infrared Spectroscopy revealed the characteristic of the functional groups viz. primary amine, carboxyl, halide, and sulfate groups present in the EPS. However, five elements (C, O, Na, S, and Ca) were detected by scanning electron microscopy - energy dispersive X-ray spectroscopy (SEM-EDX) analysis. X-ray diffraction and differential scanning calorimetric analysis confirmed the amorphous nature of EPS, which was comprised of an average particle size of 13.969 μm (*d* 0.5) with 181 nm average roughness. Two monosaccharide constituents, galactose (73.13%) and glucose (26.87%) were detected by gas chromatography–mass spectroscopy analysis. Thermal gravimetric analysis revealed that degradation of EPS obtained from *A. carterae* takes place in three steps. The EPS produced by *A. carterae* was found to be beneficial for the growth of both *A. carterae* and *Bacillus pumilus*. The potential heterogeneous properties of EPS may play an important role in harmful algal bloom.

Electronic supplementary material The online version of this article (doi:10.1007/s00248-011-9852-5) contains supplementary material, which is available to authorized users.

S. K. Mandal (✉) · R. P. Singh · V. Patel
Discipline of Marine Biotechnology and Ecology (MBE),
Central Salt and Marine Chemicals Research Institute (CSMCRI),
Council of Scientific and Industrial Research (CSIR),
G. B. Marg,
Bhavnagar 364021, India
e-mail: skmandal@csmcri.org

Introduction

The dynamics of rapid (massive) increase or almost equally decrease of phytoplankton populations is a common feature in marine plankton ecology and is known as bloom. This phenomenon generally occurs within a matter of days and also disappears just as rapidly. Harmful algal blooms (HABs) occur due to the interaction of many microorganisms like bacteria, cyanobacteria, phytoplankton (diatoms and dinoflagellates), and zooplanktons. It starts from chaotic form and reaches organized form. Later on, it is dominated by a very few microorganisms that may or may not be toxic [7]. Exopolysaccharides also play key roles in communities' succession and nutrient recycling in marine environment [34]. Many biotic and abiotic factors (temperature, pH, salinity, and nutrients like nitrate, phosphate, and silicate) trigger the harmful algal bloom formation. In this microenvironment, live cells of phytoplankton and bacteria stick to each other due to the presence of extracellular polymeric substances (EPS) that serve as biological glue and provide required stickiness for cell–cell attachment [12, 38]. The importance of microbial EPS production by bacteria [13], cyanobacteria [9], yeast [11], and basidiomycetes [8, 21] are already reported as well. However, phytoplankton cells including desmids [19], diatoms [36], and cyanobacteria [28] are also known to produce EPS into their external medium. The organic exudates become highest during the stationary growth phase of marine microorganism [18, 29].

Amphidinium carterae Hulburt 1957 is a known toxic marine dinoflagellate known to cause red tide and also reported as the causative organism for mass mortality of fish [26]. It is also listed as harmful toxic microalgae by

Intergovernmental Oceanographic Commission and United Nations Educational, Scientific and Cultural Organization (IOC-UNESCO). There are a few reports on EPS production, isolation, and characterization by some microalgae such as *Chaetoceros affinis* [25], *Cylindrotheca closterium*, *Navicula salinarum* [36], and *Dunaliella salina* [24]. In addition to the above, some other toxic phytoplankton species like *Pseudo-nitzschia* sp, *Prorocentrum* sp, *Ostrepsis* sp, *Dinophysis* sp, *Gymnodinium breve*, *Alexandrium* sp, *Gymodinium catenatum*, etc. are repeatedly reported with toxic or harmful blooms. This study investigated the characteristics of EPS produced by toxic dinoflagellate like *A. carterae* and its interaction with a bacterial test organism, *Bacillus pumilus* (NCBI accession number, HQ318731). The release of toxic substances by phytoplankton and their role in the planktonic blooms are not yet well understood and are very rare in literature [7]. In this study, we have tried to describe the species-specific interaction between *A. caterae* and *B. pumilus*, which may help to understand the role of EPS in bloom formation and/or termination.

Materials and Methods

Collection, Isolation, and Culture of Axenic *A. carterae*

A. carterae cells were isolated from Okha Port Harbour (22° 28′ 22″ N and 69° 05′ 03″ E), Okha, India. The *A. carterae* was grown in enriched seawater with Provasoli-Guillard medium with f/2 concentration. The culture was maintained under cool-white fluorescent light with the intensity of 250±10 Lux, 12:12 h light and dark cycle and at 25±1°C. The inoculum was treated with a serial dilution of 0.25%, 0.50%, and 1.0% of a mixture of antibiotics containing penicillin-G, 1 g; streptomycin sulfate, 2 g; kanamycin, 1 g; neomycin, 200 mg; and nystatin, 25 mg for 24 h. The axenicity of the *A. carterae* culture was tested by spreading the treated culture media (100 μl) onto the Zobell marine agar (2216, Himedia, India) and incubating for 10 days at 30°C (a longer period was given for the slow-growing bacterial isolates). No bacterial growth was observed even at the media containing the lowest concentration (0.25%) of antibiotic mixture. These axenic cells were used for experimental purpose. The growth curve of *A. carterae* has been determined by total cell count using Sedgwick Rafter counting chamber. The daily growth rate (DGR) was calculated using the following formula: $DGR(\%) = [(w_t/w_o)^{1/t} - 1] \times 100$, where w_t=biomass obtained during the final observation, w_o=biomass obtained during the initial observation, and t=incubation time. The isolation and characterization of *B. pumilus* has been done according to our previous reports [33].

Extraction of EPS Produced by *A. carterae*

A. carterae was harvested for EPS production in their stationary phase by centrifuging 100 ml of culture medium at 15,000×*g*, 4°C for 30 min. The cell pellets were freeze-dried and weighed. The supernatants were pressure-filtered through cellulose nitrate filters with 0.25 μm pore size (Millipore filters, Bangalore, India). EPS was precipitated from the final filtrate after the addition of three volumes of cold isopropanol, and the solution was kept overnight at 4°C. The resulting precipitate was recovered by vacuum filtration through a sintered glass apparatus. An additional 100 ml of cold isopropanol was added to the filtrate, then the solution was placed at −20°C overnight, and the precipitate, thus formed, was recovered as above. The precipitate was washed with 70–100% ethanol–water mixtures. After washing with ethanol-water mixtures, the desalted EPS was collected, then dried in desiccator and stored at room temperature until all chemical and physical analyses were performed [34].

Molecular Weight Determination of EPS

The molecular weights of samples were determined by gas permeation chromatography (GPC; Water Alliance, model 2695). Fifty microliters of 2% EPS was loaded to GPC column ultrahydrogel 120 and 500 at 40°C. Elution was monitored by a refractive index detector (2414). The column was calibrated with standard dextran (molecular weight, 5,200–668,000 kDa) from PSS, USA. Furthermore, the monosaccharide contents of EPS were estimated by alditol–acetate method [32]. Protein contents present within EPS was determined by Bradford method with BSA as standard [5].

Fourier Transformed–Infrared Spectroscopy and ^{1}H NMR Analysis

Pellets of 0.75 mg of EPS were prepared with KBr followed by pressing the mixture into a 16-mm-diameter mold. Fourier Transformed–Infrared Spectroscopy (FT-IR) spectrum was recorded on Perkin Elmer (Spectrum GX) with a resolution of 4 cm^{-1} in a 400–4,000-cm^{-1} region [39].

Noise-decoupled ^{1}H nuclear magnetic resonance (NMR) spectra were recorded on a Bruker Avance-II 200 spectrometer (Switzerland) at 200 MHz. EPS of the *A. carterae* was dissolved in the *d*-NaOH (50 mg ml^{-1}), and spectra were recorded at 25°C with 5,000–5,200 accumulations, 5.9 μs pulse duration, 1.2 s acquisition time, and 6 μs relaxation delay.

Particle Size Distributor, Energy Dispersive X-ray Spectroscopy, and Atomic Force Microscopy

Particle size distributions were measured by laser diffraction (Malvern Mastersizer 2000, Malvern Ltd., Worcestershire, UK). Elemental analysis of EPS was done using energy dispersive X-ray spectroscopy (EDX; Oxford Instruments, UK). Phase imaging atomic force microscopy (AFM) is powerful tool in the surface characterization of biomaterials, and the resulting phase image is able to detect chemical variation and reveal more detailed surface properties than a morphological image [40]. For AFM, the glass cover slips (Himedia, India) were treated with a mixture of 15 ml of HCl and 5 ml of HNO_3 for 30 min followed by treatment with a mixture of 20 ml of H_2SO_4 and 5 ml of H_2O_2 for 30 min. The cover slips was rinsed with Milli-Q and stored for AFM analysis. Samples for AFM were prepared according to Grabar et al. [14].

X-ray Diffraction and Thermal Gravimetric and Differential Scanning Calorimetric Analyses

X-ray diffraction (XRD) was performed on X-ray powder diffractometer (Philips X'pert MPD, The Netherlands) instrument equipped with a PW3123/00 curved Ni-filtered CuKα (λ=1.54056°A). Radiation generated at 40 kV and 30 mA with liquid nitrogen cooled the solid-state germanium detector to study the physical properties of EPS using slow scan in different ranges of two-theta angles (2–80°). The specimen length and irradiated length were 10 mm with receiving slit size of 0.2- and 200-mm goniometer radius. Distance between focus and divergences slit was 100 mm. Dried EPS sample was mounted on a quartz substrate, and intensity peaks of diffracted X-rays were continuously recorded with scan step time 1 s at 25°C. The *d*-spacings appropriate to diffracted X-rays at that value of θ were calculated according to Bragg's law. Crystallinity index (CI_{xrd}) was calculated from the area under crystalline peaks normalized corresponding to total scattering area [30].

Approximately 5 mg samples were used for the thermal gravimetric analysis (TGA) and differential scanning calorimetric (DSC) experiment. TG and DSC analyses were carried out by gradually raising the temperature 30–480°C and 30–540°C, respectively. TG and DSC analyses of EPS were carried out with Mettler Toledo TGA/SDTA System (Greifensee, Switzerland). The graphs (TGA and DSC) were plotted with weight loss (in percent) and heat flow vs. temperature, respectively. The activation energy (Ea) was calculated with Arrhenius equation while the enthalpy of transition (ΔH) and crystallinity of the EPS (CI_{DSC}) were calculated according to Singh et al. [34].

Interaction Study Between *A. carterae* and *B. pumilus* in Either Presence or Absence of Additional EPS

To study the interaction between *A. carterae* and *B. pumilus* in either presence or absence of additional EPS, the experimental design was as follows. The experiment was performed in 24-well (16 mm diameter, polystyrene-made, Corning Glass works, New York) plates. A1 to D1 marked wells of the multi-well tissue culture plate was inoculated with 1 ml of *A. carterae* containing 5,000±50 numbers of cells and served as control. A2 to D2 were used as bacterial control and inoculated with 55×10^3 colony forming unit (CFU) ml^{-1} of *B. pumilus*. A3 to D3 were inoculated with 5,000±50 number of cells ml^{-1} *A. carterae* and 10 mg of EPS. A4 to D4 were inoculated with 55×10^3 CFU ml^{-1} of *B. pumilus* and 10 mg of EPS. A5 to D5 were inoculated with 5,000±50 number of cells ml^{-1} *A. carterae* and 55×10^3 CFU ml^{-1} of *B. pumilus*. A6 to D6 were inoculated with 5,000±50 number of cells ml^{-1} *A. carterae*, 55×10^3 CFU ml^{-1} of *B. pumilus*, and 10 mg of EPS. The experiment was run within an incubator having controlled conditions, i.e., 25±0.5°C, light intensity 15 μmol photon m^{-1} s^{-1}, and 12:12 h light/dark cycles. Daily growth in terms of increase in total number of count of *A. carterae* cells was observed using Sedgwick Rafter counting chamber. The total CFU count of *B. pumilus* was carried out by spreading over 100 μl of inoculums on Zobell marine agar media after every 48-h interval.

Results and Discussion

Growth Study and EPS Production by *A. carterae*

The different growth conditions for *A. carterae* have been reported by several authors focusing on temperature, light intensity, nutrients, and vitamin requirements [16]. The growth rate of *A. carterae* followed exponential growth curve in the Provasoli-Guillard (f/2) medium at 25±1°C. The maximum cell count (68,800±283 cells ml^{-1}) was observed on the 16th day of incubation (Fig. 1). For the first 8 days, the growth rate was slow (growth rate=33%), and in the next 8 days, the growth rate was increased to 46% and reached the maximum number of cells. Thereafter, the DGR was decreased and became negative (growth rate=−3%). One-month-old culture was taken for EPS isolation, estimation, and characterization. One hundred milliliters of such culture containing 1 g cells (dry weight) of *A. carterae* produced 480 mg dry weight (lyophilized) of EPS, which is quite more as compared with *Cylindrotheca clostridium* (4.3 μg ml^{-1}) reported by Staats [36]. There are different detailed methods involved for extraction and isolation of EPS produced by different microorganisms

based on their nature of the EPS [10, 36]. However, the amount of production of EPS always depends on the different controlling factors like nutrient depletion, cell physiology, and changes in growth conditions and/or bacterial–phytoplankton interactions.

Determination of Molecular Mass

Generally, the molecular mass of EPS has been reported to range from 20 to 2,000 kD [1, 23]. The extracted EPS of *A. carterae* was applied to GPC to determine their molecular masses. GPC revealed two chromatographic peaks corresponding to fractions, 233 and 1,354 kDa with 1.195 and 1.107 polydispersity, respectively (Supplementary Fig. 1).

FT-IR, ^{1}H NMR, and Monosaccharide Analysis

FT-IR analysis revealed the presence of carbohydrate in the EPS produced by *A. carterae*. The presence of hydroxyl groups into the EPS is indicated by two peaks at 2,926 and 3,407 cm^{-1} and another peak at 1,650 cm^{-1} indicated that the EPS produced by *A. carterae* consists of more than one monosaccharide [6]. A symmetrical stretched peak near 1,513 cm^{-1} indicated the presence of carboxyl groups. The prominent absorption observed at 1,650 cm^{-1} was attributed to the stretching vibration of C=O and C−N. The strong absorption at 1,117 cm^{-1} revealed the presence of sulfate groups as S=O and C−O−S in the EPS of *A. carterae* [28]. This sulfate group may provide anionic nature to EPS [27]. Presence of glycosidic linkage bond could be determined with the peaks of 614 and 461 cm^{-1} (Fig. 2). The FT-IR spectra of the polymer evidenced the presence of carboxyl groups, which may serve as binding sites for divalent cations. In addition, the presence of S=O, C−O−S, and carboxyl groups could be responsible for binding of more water molecules and contributed to more weight loss in the TGA. The presence of various functional groups in the EPS produced by *A. carterae* revealed its structural complexity.

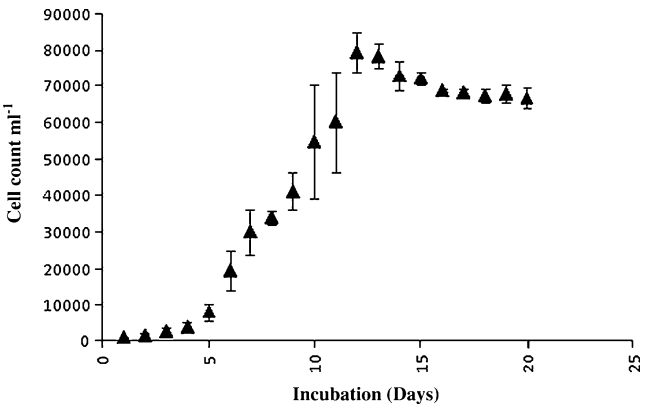

Figure 1 Growth of *A. carterae*

The ^{1}H NMR spectrum showed 12 anomeric signals for the EPS produced by *A. carterae* (Fig. 3) depicting its complex and heterogeneous nature. The complex nature of the biopolymer produced by *A. carterae* was further concluded by convergence of signals in the region of δ 3.7–3.9 ppm. The signals around δ 1.0–1.258 ppm arise from the methyl protons of the 6-deoxy sugars [22]. The signal around δ 2.02 ppm confirmed the presence of acetyl groups linked to different sugars in EPS.

In the diatoms, normally secreted EPS is composed predominantly of glucose with minor quantities of other sugars and it is reported that 23% and 42% of EPS-containing glucose present in *N. salinarum* and *C. closterium*, respectively [35]. Galactose was also an important component sugar in granular EPS. In the present study, GC-MS analysis showed the presence of galactose (73.13%) and glucose (26.87%) in the EPS of *A. carterae* (Supplementary Fig. 2) while other sugars arabinose, mannose, rhamnose, and xylose could not be detected. To the best of our knowledge, it is the first report of the monosaccharide analysis of a toxic marine dinoflagellate. The amount of protein was found to be 3 μg in 1 mg of EPS.

Energy Dispersive X-ray Spectroscopy, Particle Size Distributor, and AFM Analysis

EPS constituted of varied particle sizes from 2.753 (*d* 0.1) to 43.845 (*d* 0.9) μm with an average size of 13.969 μm (*d* 0.5) and 1.0945 m^2 g^{-1} specific surface areas (Fig. 3 and Supplementary Fig. 3). Quantitative elemental analysis was done by SEM-EDX, which revealed the weight and atomic percentage of different elements present (C, O, Na, S, and Ca) in the EPS produced by *A. carterae*. The results have been depicted in Table 1, and the graphical representation has been given as Supplementary Fig. 4.

The different particle size within EPS showed the height distribution profiles of the surface roughness (Fig. 4). Roughness average was 181 nm, and histogram of the AFM analysis showed the distribution profile of particle within EPS on the cover slide. The height histogram revealed that the distribution of the EPS particle maximum in the center of the cover slips. To best of our knowledge, it's the first report of the energy dispersive X-ray spectroscopy, particle size distributor, and AFM analysis of a toxic marine dinoflagellate.

X-ray Diffraction (XRD), TG, and DSC Analyses

The XRD profile of EPS obtained from *A. carterae* exhibited the characteristic diffraction peaks at 32.1° and 48.7° with inter-planar spacing (*d*-spacing) 2.788 and

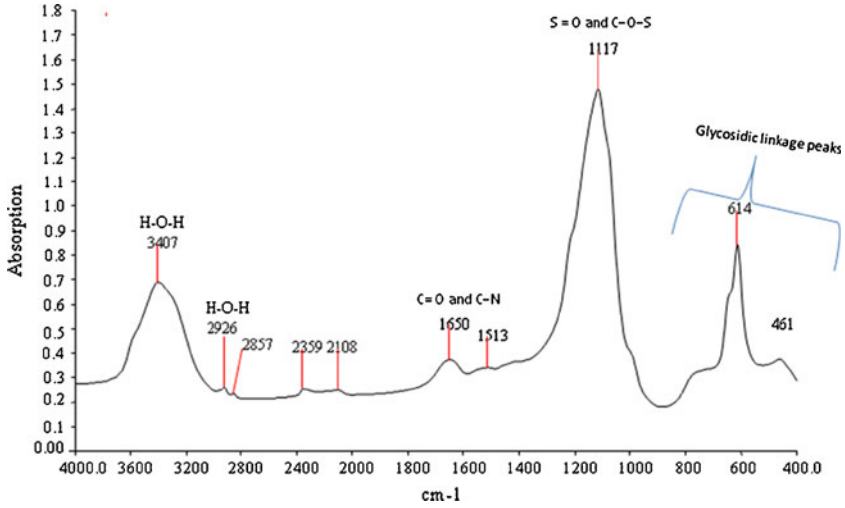

Figure 2 FT-IR analysis of EPS produced by *A. carterae*

1.867 A°, respectively (Fig. 5 and Supplementary Fig. 5). XRD pattern predicted that EPS is amorphous in nature with 0.121 crystallinity index. Crystalline parts give sharp narrow diffraction peaks while amorphous component gives a broad peak. It is difficult to interpret broad amorphous peaks of several amorphous EPS in X-ray scattering profile [31]. The ratio between sharp narrow diffraction peaks and broad peaks was used to calculate the amount of crystallinity in the EPS produced by *A. carterae*.

TGA was carried out dynamically between weight loss vs. temperatures and experimental result showed in Fig. 6. TGA showed that degradation of EPS obtained from *A. carterae* takes place in three steps. Eighty-one percent of total EPS weight loss recorded within 30°C to 180°C might be due to presence of a large number of water molecules and also a high level of carboxyl group in the EPS. According to Kumar et al. [20], there is a greater increase in the degradation of the first phase because high levels of carboxyl groups are bound to more water molecules. More than 180°C was required for degrading the rest 19% of the EPS. In the second phase of degradation, 13% of weight loss was observed between 180°C to 380°C, and thereafter, the remaining complete degradation takes place in the final steps between 380°C to 500°C.

Crystallization temperature transition is an exothermic process, and DSC analysis of EPS produced by *A. carterae* showed a significant thermal transition. DSC thermogram showed two distinct exothermic peaks of EPS with crystallization temperature (T_c) 116.51°C (onset temperature, 112.58°C) and 2,042.58 mJ latent energy, respectively (Fig. 7). The melting peaks were found at 217.17°C (onset temperature, 221.95°C) with 120.62 mJ latent energy for T_m. The activation energy (*n*th order of reaction) of exothermic transitions was 79.41±1.07 (T_c), and 589.13±2.78 (T_m)kJ mol^{-1} for endothermic transition. The endothermic reaction of the EPS of *A. carterae* required more energy than exothermic reaction. The DSC analysis showed the 11% crystallization (CI_{xrd} 0.11) and revealed the EPS of *A. carterae* as amorphous in nature. In contrast with XRD, approximately equal crystalline index (12.1) was observed for EPS from DSC thermogram and

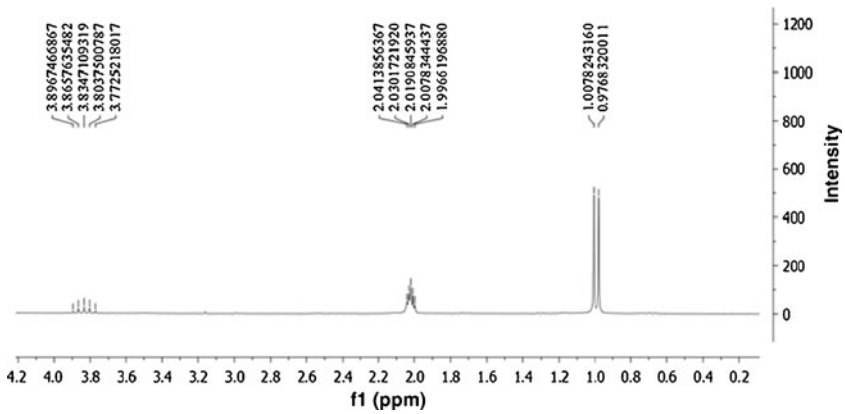

Figure 3 ^{1}H NMR of EPS obtained from *A. carterae*

Table 1 Elemental EDX micro-analysis of EPS obtained from *A. carterae*

Element	Standard	Weight%	Atomic%
C	$CaCO_3$	39.84	47.82
O	SiO_2	54.89	49.45
Na	Albite	2.44	1.53
S	FeS_2	1.98	0.89
Ca	Wollastonite	0.85	0.31
Total		100	

Data are expressed with weight and atomic percents

Number of iterations=3

same variation may be because of uncertainties in placing base line for area integration.

Interaction between *A. carterae* and *B. pumilus* in Presence and Absence of EPS

In the present study, it was found that EPS produced by *A. carterae* induce the growth of bacterial isolate, *B. pumilus* and *A. carterae* itself. The maximum growth of bacterial isolate in terms of CFU count (62×10^9 CFU ml^{-1}) was observed in presence of EPS of *A. carterae*. However, the minimum growth of bacterial isolate (25×10^6 CFU ml^{-1}) was observed in the co-culture of bacteria isolate and *A. carterae* without addition of EPS. Inhibiting the CFU count of *B. pumilus* in co-culture (without addition of EPS) suggested the allelopathy action of *A. carterae.* On the contrary, the maximum growth of *A. carterae* in terms of total cell count (77×10^3 cells ml^{-1}) was observed in the presence of EPS while the same was minimum (32×10^3 cells ml^{-1}) in co-culture of bacteria isolate and *A. carterae* in presence of EPS. The growth of bacterial isolate and *A. carterae* was increased in the presence of EPS, which revealed that the EPS produced by the *A. carterae* acts as a nutrient supplement. Bacterial action on components of the organic matter produced by the vicinity of phytoplankton influences carbon and nutrient fluxes in various pathways: microbial loop, sinking, grazing food chain, storage, and fixation [2]. The *A. carterae* showed the negative impact on the growth of bacterial isolate. The minimum CFU count of bacterial cells observed in the presence of *A. carterae* supports the previous statement (Fig. 8). The co-culture of bacterial isolate and *A. carterae* along with EPS obtained low CFU count. Initially, it might be due to biotic stress of toxic *A. carterae*, and later on, CFU count increased rapidly due to the positive impact of EPS after 8 days and the observed exponential growth. Most opportunistic bacteria

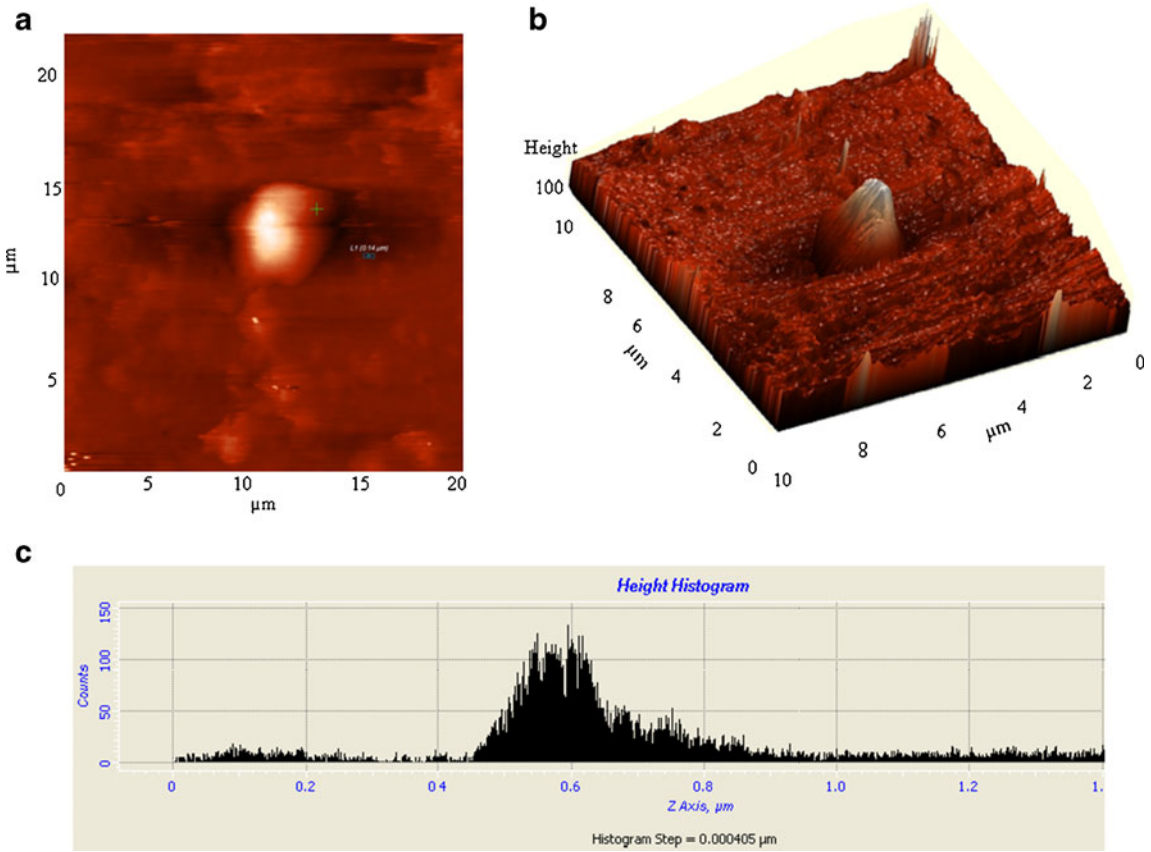

Figure 4 AFM analysis [two- (**a**), three-dimensional view (**b**), and histogram (**c**)] of EPS and EPS distribution on the cover slip

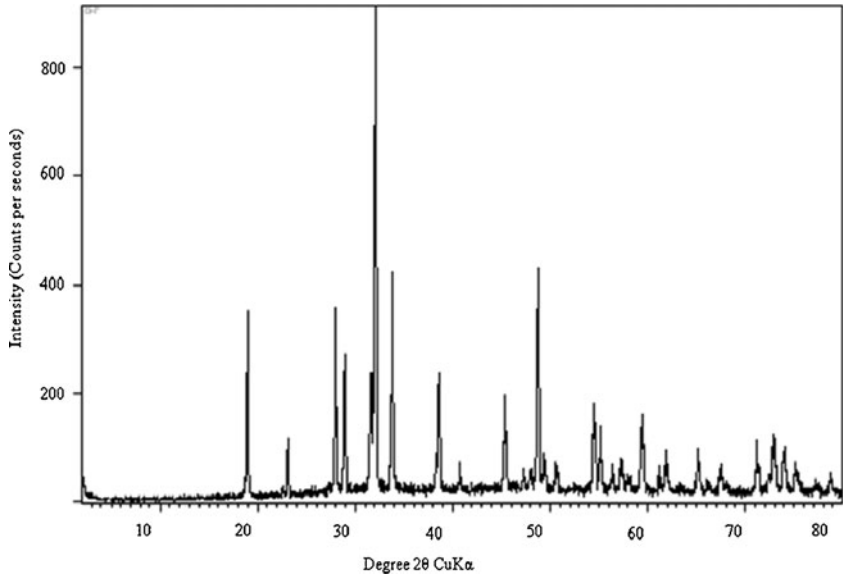

Figure 5 XRD profile of EPSs isolated from *A. carterae*

have a repertoire of hydrolytic enzymes which allows them to efficiently utilize EPS such as phytoplankton exudates [22]. Thus, the distribution of bacterial number and diversity in the marine environment may be controlled by its hydrolytic enzyme activity. Co-culture (*A. carterae* and *B. pumilus*) without EPS showed similar growth pattern as observed in co-culture with EPS, but total cell count per milliliter was observed less in comparison to co-culture without EPS throughout the experiment. Here, the interesting result observed was that the total cell count per milliliter was less in the co-culture with EPS and may be due to competition for nutrient and space between both species. In the co-culture (Bac-Dino-EPS), the growth rate of *B. pumilus* was initially inhibited due to toxic effect of *A. carterae* and revealed low count. After acclimatization of the bacteria towards the toxic effect of *A. carterae*, it was increased with exponential growth and maximum nutrient and space occupied by the bacterial isolates in the presence of EPS, so the growth of *A. carterae* was inhibited by less nutrient and space, but showing the general patterns of growth during incubation (Fig. 8). On the other hand, *A. carterae* showed maximum growth (77×10^3 cells ml^{-1}) in the presence of additional EPS followed by the co-culture (63×10^3 cells ml^{-1}) of *A. carterae* and *B. pumilus* without EPS as compared with control (10×10^3 cells ml^{-1}). *A. carterae* showed initially higher growth (41×10^3 cells ml^{-1}) in the control and decreased with time, i.e., on the sixth and eighth days, the total cell counts being 35×10^3 cells ml^{-1} and 10×10^3 cells ml^{-1}, respectively. However, in the presence of EPS, *A. carterae* showed exponential growth throughout the experiment. In the *A. carterae* and *B. pumilus* interaction study, regeneration of *A. carterae* by

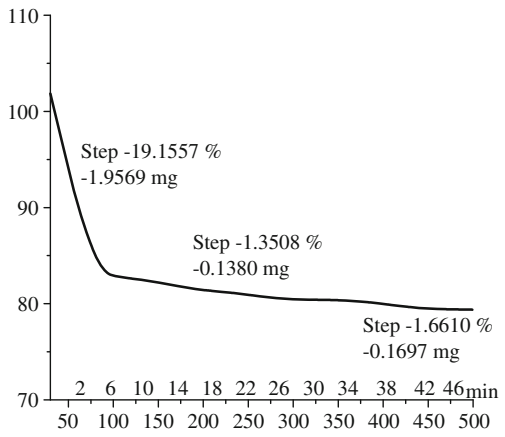

Figure 6 TG thermogram of EPS obtained from *A. carterae* at heating rate of 10°C

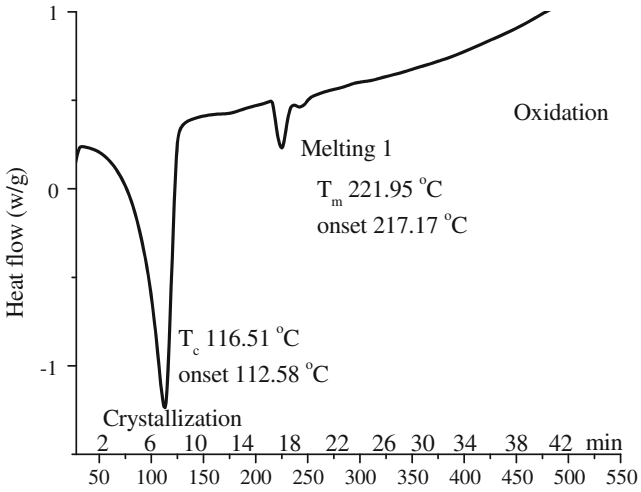

Figure 7 DSC thermogram of EPS obtained from *A. carterae* at heating rate of 10°C

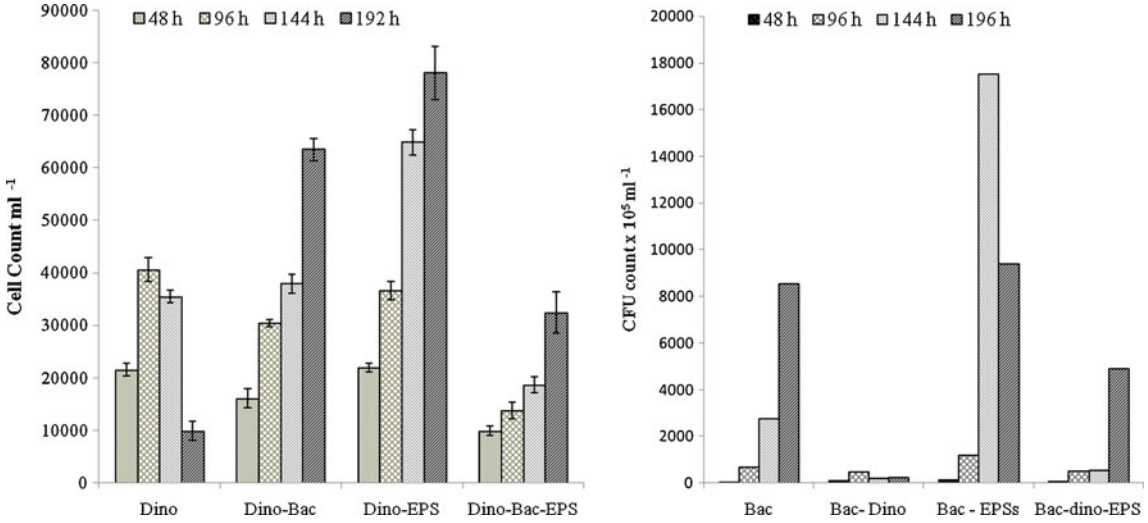

Figure 8 Growth competition and interaction study between *A. carterae* and *B. pumilus*. **a** Total cell count of *A. carterae* in the presence of either *B. pumilus* or EPS and both. **b** CFU of *B. pumilus* count in the presence of either *A. carterae* or EPS and both. The value of the *bar* (Bac-EPS on 192 h) is represented as 100 times less

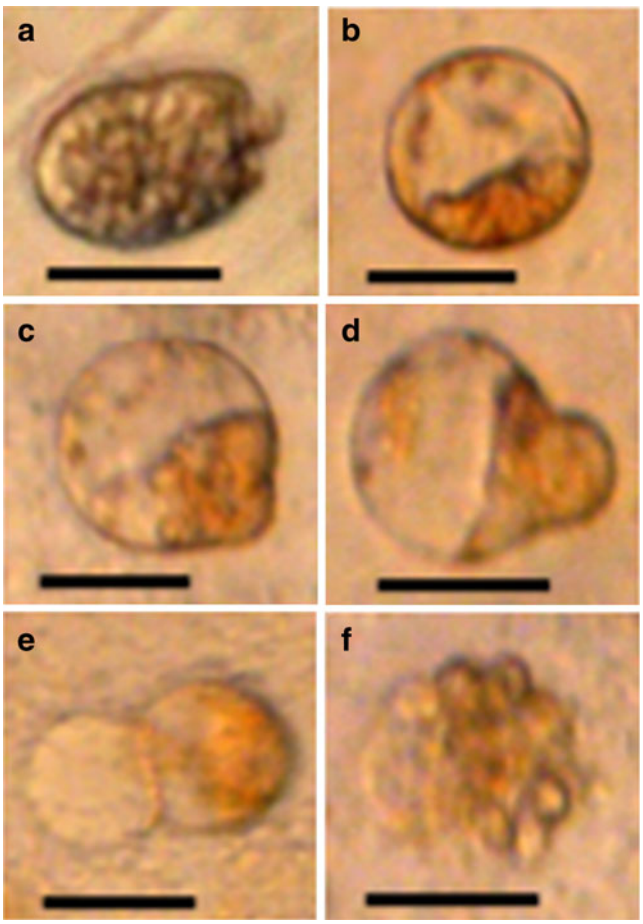

Figure 9 Budding activities of *Amphidinium cartilage* was observed during the interaction between *B. pumilus* and *A. carterae.* **a** Original cup-shape of the test organism, **b** round shape of the test organism, **c** initiation of bud formation, **d** growing stage, **e** transformation of cytoplasmic material to the new bud, **f** releasing of bud, and degradation of the mother cell. Scale, 10 μm

budding activities was also observed (Fig. 9), which might be the first report of asexual reproduction of *A. carterae*. This budding activity observed in the co-culture of *A. carterae* and *B. pumilus* in the presence of EPS might be due to physiological stress generated in the presence of *B. pumilus*. Dissolved free and combined carbohydrate concentrations have also been reported from phytoplankton bloom [17]. During natural phytoplankton blooms, extracellular algal products can stimulate bacterial growth and activity [3, 35]. The high hydrolytic activities of bacteria-colonizing phytoplankton cells of macroscopic organic aggregates led to 'uncoupled solubilization' of EPS which reduced the sinking flux [15, 35] and helped these to float on the seawater surface during HABs formation.

Probable Role of EPS Produced by *A. carterae* in Harmful Algal Bloom

In the marine environment, EPS produced by microorganism help to form biofilm, and unicellular or multicellular aggregates that increase cell-to-cell contact and the sequestering of nutrients and thus provide protection and survivability [4, 27]. Vardi et al. [37] reported that allelopathic compounds produced by phytoplankton become active in succession events [37]. In the *A. carterae* and *B. pumilus* interaction study, it was observed that the growth of *B. pumilus* was less in the co-culture of *B. pumilus* with *A. carterae* (without additional EPS) as compared with the co-culture of *B. pumilus* with *A. carterae* (with additional EPS). The EPS might have played role for *B. pumilus* succession after 196 h of incubation (Fig 8). In this interaction study, the growth of bacterial isolates was suppressed might be due to allelopathic

interaction, i.e., toxin production by *A. carterae*. *A. carterae* produces hemolysins, which are low-molecular-weight compounds believed to be involved in fish mortality. There are also five types of hemolysins and hemolysins 3, 4, and 5 are more potentially toxic than 1 and 2 [26]. Here, the hemolysins may be responsible for restriction of the growth of the *B. pumilus*. Bacterial isolates gets acceleration in growth after 196 h due to EPS only. The distribution of cations such as Na and Ca in the EPS detected in the EDX suggest their binding to the negative charges of the sulfate groups might have helped in *B. pumilus* growth. In addition, the sulfate present as a functional group in the EPS confers its anionic character in the marine environment. In a natural marine environment, the nutrients can interact with EPS in order to increase availability of elements and help to concentrate the dissolved organic compounds [27]. Thus, EPS can play an important role in the succession of algal bloom forming organism and/or it may terminate the bloom by increasing the growth of decomposers.

Conclusion

There is little information on the ecological function of the EPS produced by toxic dinoflagellates in the marine environment. In the detailed information in relation to the isolation and characterization of the EPS produced by *A. carterae*, a toxic dinoflagellate has been described. The EPS produced by *A. carterae* is complex in nature. The various functional groups like amine, carboxyl, halide, and sulfate present in the EPS, as revealed by FT-IR and ^{1}H NMR, and the further five elements (C, O, Na, S, and Ca), as detected with SEM-EDX, may be attached with hydroxyl and/or carboxyl groups of glucose and galactose. These EPS are composed of different of molecular weights (233 and 1,354 kDa) as these can be seen with AFM analysis. Amorphous nature of these EPS is confirmed with the XRD and DSC. The physical and chemical properties of the EPS produced by *A. carterae*, and its probable role in harmful algal bloom formation / termination, which is described here may be useful for comparing with the EPS produced by other phytoplankton including dinoflagellate, which may lead better understanding of the *allelopathic* interaction occurred in microbial environment.

Acknowledgments The authors are thankful to Dr. B. Rabari, Mr. H. Gupta, Mr. V. Agarwal, and Mrs. P. Bhatt, Analytical Section, CSMCRI, for their enormous help during sample analysis. The authors are also thankful to Ms. D. Jain and Mr. I. Puncha for their help during sample collection. The work was supported by NWP 0018, Council of Scientific and Industrial Research, New Delhi, and SAC-CSMCRI collaborative project (GAP 1049).

References

1. Arias S, Moral AD, Ferrer MR, Tallon R, Quesada E, Bejar V (2003) Mauran, an exopolysaccharide produced by the halophilic bacterium *Halomonas maura*, with a novel composition and interesting properties for biotechnology. Extremophiles 7:319–326
2. Azam F (1998) Microbial controls of oceanic carbon flux: the plot thickens. Science 280:694–696
3. Bell WH, Lung JM, Mitchell R (1974) Selective stimulation of marine bacteria by algal extracellular products. Biol Bull 143:265–277
4. Bhaskar PV, Bhosle NB (2005) Microbial extracellular polymeric substances in marine biogeochemical processes. Curr Sci 88(1):10
5. Bradford MM (1976) A rapid and sensitive method for the quantification of microgram quantities of protein utilizing the principle protein–dye binding. Anal Biochem 72:248–254
6. Bremer PJ, Geesey GG (1999) An evaluation of biofilms development utilizing non-destructive attenuated total reflectance Fourier transform infrared spectroscopy. Biofouling 3:89–100
7. Chattopadhyay J, Sarkar RR, Abdllaoui AE (2002) A delay differential equation model on harmful algal blooms in the presence of toxic substances. IMA J Math Appl Med Biol 19:137–161
8. Chi Z, Zhao S (2003) Optimization of medium and cultivation conditions for pullulan production by new pullulan-producing yeast. Enzyme Microb Tech 33:206–211
9. De-Philippis R, Sili C, Paperi R, Vincenzini M (2001) Exopolysaccharide producing cyanobacteria and their possible exploitation: a review. J Appl Phycol 13:293–299
10. Domozych DS, Kort S, Benton S, Yu T (2005) The extracellular polymeric substance of the green alga *Penium margaritaceum* and its role in biofilm formation. Biofilms 2:129–144
11. Duan X, Chi Z, Wang L, Wang X (2008) Influence of different sugars on pullulan production and activities of a-phosphoglucose mutase, UDP-Gpyrophosphorylase and glucosyltransferase involved in pullulan synthesis in *Aureobasidium pullulans* Y68. Carbohyd Polym 73:587–593
12. Engel A (2000) The role of transparent exopolymer particles (TEP) in the increase in apparent particle stickiness (α) during the decline of a diatom bloom. J Plankton Res 22:485–497
13. Freitas F, Alves VD, Pais J, Costa N, Oliveira C, Mafra L, Hilliou L, Oliveira R, Reis MA (2009) Characterization of an extracellular polysaccharide produced by a *Pseudomonas* strain grown on glycerol. Bioresource Technol 100:859–865
14. Grabar KC, Freeman RG, Hommer MB, Natan MJ (1995) Preparation and characterization of Au colloid monolayers. Anal Chem 67(4):735–743
15. Grossart HP, Simon M (1998) Bacterial colonization, microbial decomposition of limnetic organic aggregates (lake snow). Aquat Microb Ecol 15:115–125
16. Ismael AA, Halim Y, Kalil A (1999) Optimum growth conditions for *Amphidinium carterae* Hulburt from eutrophic waters in Alexandria (Egypt) and its toxicity to the brine shrimp *Artemia salina*. Grana 38:179–185
17. Ittekkot V, Brockmann U, Michaelis W, Degen ET (1981) Dissolved free and combined carbohydrates during a phytoplankton bloom in the northern North Sea. Mar Ecol Prog Ser 4:299–305
18. Khandeparkar RDS, Bhosle NB (2001) Extracellular polymeric substances of the marine fouling diatom *Amphora rostrata* Wm. Sm. Biofouling 17:117–127
19. Kiemle SN, Domozych DS, Gretz MR (2007) The extracellular polymeric substances of desmids (Conjugatophyceae, Streptophyta): chemistry, structural analyses and implications in wetland biofilms. Phycologia 46(6):617–627
20. Kumar CG, Joo HS, Choi JW, Koo YM, Changa CS (2004) Purification and characterization of an extracellular polysaccha-

ride from haloalkalophilic *Bacillus* sp. I-450. Enzyme Microb Technol 34:673–681
21. Manzoni M, Rollini M (2001) Isolation and characterization of the exopolysaccharide produced by *Daedalea quercina*. Biotechnol Lett 23:1491–1497
22. Martinez J, Smith DC, Steward GF, Azam F (1996) Variability in ectohydrolytic enzyme activities of pelagic marine bacteria and its significance for substrate processing in the sea. Aquat Microb Ecol 10:223–230
23. Mata JA, Bejar V, Llamas I, Arias S, Bressollier P, Tallon R, Urdaci MC, Quesada E (2006) Exopolysaccharides produced by the recently described bacteria *Halomonas ventosae* and *Halomonas anticariensis*. Res Microbiol 157:827–835
24. Mishra A, Jha B (2009) Isolation and characterization of extracellular polymeric substances from micro-algae *Dunaliella salina* under salt stress. Bioresource Technol 100:3382–3386
25. Myklestad SM, Haug A (1972) Production of carbohydrates by the marine diatom *Chaetoceros affinis* var. *willei* (Gran) Hustedt. II. Preliminary investigation of the extracellular polysaccharide. J Exp Mar Biol Ecol 9:137–144
26. Nayak BB, Karunasagar I, Karunasagar I (1997) Infuence of bacteria on growth and hemolysin production by the marine dinoflagellate *Amphidinium carterae*. Mar Biol 130:35–39
27. Nichols CM, Lardiere SG, Bowman JP, Nichols PD, Gibson JAE, Guezennec J (2005) Chemical characterization of exopolysaccharides from Antarctic marine bacteria. Microb Ecol 49:578–589
28. Parikh A, Madamwar D (2006) Partial characterization of extracellular polysaccharides from cyanobacteria. Bioresource Technol 97:1822–1827
29. Pavlova K, Grigorova D (1999) Production and properties of exopolysaccharide by *Rhodotorula acheniorum* MC. Food Res Intl 32:473–477
30. Ricou P, Pinel E, Juhasz N (2005) Temperature experiments for improved accuracy in the calculation of polyamide-11 crystallinity by X-ray diffraction. Advances in X-ray Analysis International Centre for Diffraction Data
31. Shimazu A, Miyazaki T, Ikeda K (2000) Interpretation of d-spacing determined by wide angle X-ray scattering in 6 FDA-based polyimide by molecular modelling. J Membrane Sci 166:113–118
32. Siddhanta AK, Goswami AM, Shanmugam M, Mody KH, Ramavat BK, Mahir OP (2001) Water soluble polysaccharide of marine algae species *Ulva* (Ulvales, Chlorophyta) of Indian waters. Ind J Mar Sci 30:166–172
33. Singh RP, Mantri VA, Reddy CRK, Jha B (2011) Isolation of seaweed associated bacteria and their morphogenesis inducing capability in axenic cultures of the green alga *Ulva fasciata*. Aquat Biol 12(1):13–21
34. Singh RP, Shukla MK, Mishra A, Kumari P, Reddy CRK, Jha B (2011b) Isolation and characterization of exopolysaccharides from seaweed associated bacteria *Bacillus licheniformis*. Carbohyd Polym 84:1019–1026
35. Smith DC, Steward GF, Long RA, Azam F (1995) Bacterial mediation of carbon fluxes during a diatom bloom in a mesocosm. Deep-Sea Res-II 42:75–97
36. Staats N, de Winder B, Stal LJ, Mur LR (1999) Isolation and characterization of extracellular polysaccharides from the epipelic diatoms *Cylindrotheca closterium* and *Navicula salinarum*. Eur J Phycol 34:161–169
37. Vardi A, Schatz D, Beeri K, Motro U, Sukenik A, Levine A, Kaplan A (2002) Dinoflagellate–cyanobacterium communication may determine the composition of phytoplankton assemblage in a mesotrophic lake. Curr Biol 12(20):1767–1772
38. Vieira AAH, Ortolano PIC, Giroldo D, Oliveira MJD, Bittar TB, Lombardi AT, Sartori AL (2008) Role of hydrophobic extracellular polysaccharide of *Aulacoseira granulate* (Bacillariophyceae) on aggregate formation in a turbulent and hypereutrophic reservoir. Limnol Oceanogr 53(5):1887–1899
39. Wang Y, Zhang M, Ruan D, Shashkov AS, Kilcoyne M, Savage AV, Zhang L (2004) Chemical components and molecular mass of six polysaccharides isolated from the sclerotium of *Poria cocos*. Carbohyd Res 339:327–334
40. Ye Z, Zhao X (2010) Phase imaging atomic force microscopy in the characterization of biomaterials. J Microscopy 238(1):27–34